

JAAS

Accepted Manuscript



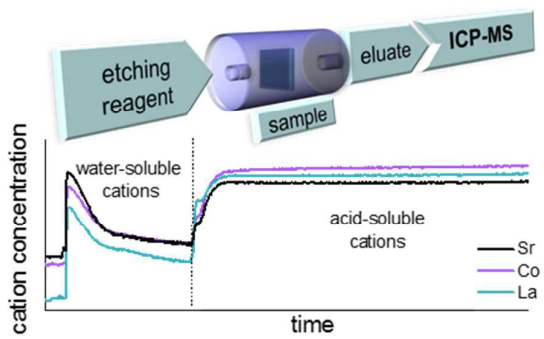
This is an *Accepted Manuscript*, which has been through the Royal Society of Chemistry peer review process and has been accepted for publication.

Accepted Manuscripts are published online shortly after acceptance, before technical editing, formatting and proof reading. Using this free service, authors can make their results available to the community, in citable form, before we publish the edited article. We will replace this *Accepted Manuscript* with the edited and formatted *Advance Article* as soon as it is available.

You can find more information about *Accepted Manuscripts* in the [Information for Authors](#).

Please note that technical editing may introduce minor changes to the text and/or graphics, which may alter content. The journal's standard [Terms & Conditions](#) and the [Ethical guidelines](#) still apply. In no event shall the Royal Society of Chemistry be held responsible for any errors or omissions in this *Accepted Manuscript* or any consequences arising from the use of any information it contains.

1 Table of Contents entry



2

3

1
2
3 1 **Dynamic etching of soluble surface layers with on-line Inductively Coupled**
4 **Plasma Mass Spectrometry detection – a novel approach for determination of**
5 **complex metal oxide surface cation stoichiometry**
6
7

8
9
10 5 Andreas Limbeck^{a,*,‡}, Ghislain M. Rupp^{a,*,‡}, Markus Kubicek^a, Helena Téllez^b, John
11 Druce^b, Tatsumi Ishihara^b, John A. Kilner^{b,c} and Jürgen Fleig^a
12
13

14
15 ^a Institute of Chemical Technologies and Analytics, TU Wien, Getreidemarkt 9/164,
16 1060 Vienna, Austria
17

18 ^b International Institute for Carbon-Neutral Energy Research, Kyushu University,
19 744, Motooka Nishi-ku, Fukuoka, 819-0395, Japan
20

21 ^c Department of Materials, Imperial College London, South Kensington Campus,
22 London, SW7 2AZ, UK
23
24

25
26 [‡] A. Limbeck and G. M. Rupp contributed equally to this work
27
28

29
30 * Correspondence: Institute of Chemical Technologies and Analytics, TU Wien,
31 Getreidemarkt 9/164, 1060 Vienna, Austria. Tel.: +43 1 58801 15180. E-mail
32 addresses: A.Limbeck@tuwien.ac.at (A. Limbeck), ghislain.rupp@tuwien.ac.at (G.M.
33 Rupp)
34
35
36

37
38 22 **Abstract**
39

40
41 23 In this work, an innovative approach for determining the surface stoichiometry of
42 complex metal oxide (CMO) thin films is presented. The procedure is based on
43 treatment of the sample surface with different etching solutions, followed by on-line
44 analysis of the derived eluates using inductively coupled plasma – mass
45 spectrometry (ICP-MS). Via consecutive treatment of the sample surface with water
46 and diluted HCl, a differentiation between water soluble and acid soluble parts of
47 near surface regions in thin films is enabled. The developed procedure was applied
48 for the analysis of dense La_{0.6}Sr_{0.4}CoO_{3-δ} (LSC) thin films indicating the presence of a
49 water soluble Sr-rich phase with sub nm- thickness on top of the LSC films. The step-
50
51
52
53
54
55
56
57
58
59
60

1
2
3 32 wise optimization of this technique is reported and the results are compared to
4
5 33 measurements performed by low-energy ion scattering (LEIS). The detrimental effect
6
7 34 of the water soluble Sr rich phase on the oxygen exchange activity of LSC thin film
8
9 35 electrodes is verified by electrochemical impedance spectroscopy (EIS).
10

11 36

12
13
14 37 Keywords: Dynamic etching procedure, ICP-MS, flow injection, thin film analysis, low-
15
16 38 energy ion scattering, electrochemical impedance spectroscopy
17

18 39

20 40 INTRODUCTION

21
22
23 41 Complex metal oxides (CMOs) are key materials in an increasing number of
24
25 42 applications. Among the numerous crystal structures adopted by CMOs, those in the
26
27 43 perovskite-type (ABO_3) family have received the greatest attention followed by spinel-
28
29 44 type (AB_2O_4) and pyrochlore-type ($A_2B_2O_7$) structures. The growing interest over the
30
31 45 past decades for these and other structures can be attributed to the functional
32
33 46 diversity due to the wide range of properties that they can adopt ¹. For example, in
34
35 47 the fields of solid state electrochemistry and heterogeneous catalysis, complex metal
36
37 48 oxides are attractive alternatives to expensive noble metal catalysts ²⁻⁴. For both
38
39 49 disciplines, excellent knowledge of the structure and composition of the investigated
40
41 50 material at the reaction sites, i.e. in most applications the solid/gas phase boundary
42
43 51 (surface), is required for understanding reaction mechanisms and tailoring properties.
44
45 52 Nanoscaled systems (e.g. nanoparticles, thin films) may not only improve
46
47 53 functionalities but are also indispensable to increase the surface/bulk ratio for a
48
49 54 detailed analysis of the region of interest. Particularly, thin film model systems,
50
51 55 mostly deposited by physical and chemical vapor deposition techniques, offer the
52
53 56 possibilities for using a large variety of analytical methods to characterize the surface
54
55 57 and near surface region as well as depth profiling the layers beneath.
56
57
58
59
60

1
2
3 58 Imaging methods, such as atomic force and scanning tunneling microscopy,
4
5 59 are widely used to characterize the structure of the termination layer. For the analysis
6
7 60 of the chemical composition, X-ray photoelectron spectroscopy (XPS) and Auger
8
9 61 electron spectroscopy (AES) or ion bombardment techniques such as secondary ion
10
11 62 mass spectrometry (SIMS), Rutherford backscattering (RBS) and low energy ion
12
13 63 scattering (LEIS) are often applied ⁵. However, quantification of the exact surface
14
15 64 composition by these techniques is non-trivial. Alternative methods for quantitative
16
17 65 analysis of thin films are glow-discharge mass spectrometry (GDMS) ^{6, 7} or laser-
18
19 66 ablation inductively coupled plasma mass spectrometry (LA-ICP-MS) ^{8, 9}. These and
20
21 67 other well-established techniques also enable the analysis of depth profiles with
22
23 68 sufficient sensitivity and depth resolution.

24
25
26
27 69 Application of these analytical tools has already shown that for complex metal
28
29 70 oxides the structure and composition at and close to the surface frequently differ from
30
31 71 the bulk. Elastic and electrostatic forces may drive segregation of dopants to the
32
33 72 surface of CMOs ^{10, 11}, reactions between gas phase and solid may lead to the
34
35 73 formation of secondary phases ^{12, 13}, and exsolution of metallic particles on the
36
37 74 surface of perovskites is found under reducing conditions ^{14, 15}, to mention only a few
38
39 75 examples. These changes are crucial for the (electro-)catalytic activity of the
40
41 76 materials and their analysis requires methods that are specifically adapted to these
42
43 77 complex phenomena. One example of a particularly challenging situation is given for
44
45 78 the perovskite-type CMO $\text{La}_{0.6}\text{Sr}_{0.4}\text{CoO}_{3-\delta}$ (LSC). LSC is a promising cathode
46
47 79 material for intermediate temperature solid oxide fuel cells due its high activity for the
48
49 80 surface oxygen exchange ¹⁶⁻¹⁸. However, degradation of the surface activity under
50
51 81 various conditions is reported in the literature and several correlations to structural
52
53 82 and/or compositional changes of the electrode surface have been reported ^{19, 20}.
54
55 83 Chemical investigations on thin LSC films using XPS, SIMS and inductively coupled
56
57
58
59
60

1
2
3 84 plasma – optical emission spectrometry (ICP-OES) already revealed an
4
5 85 accumulation of Sr at the electrode surface, which may be responsible for the
6
7 86 deactivation of the oxygen reduction reaction ²¹⁻²³. Furthermore, Cai et al. ²³
8
9
10 87 proposed a secondary Sr phase such as SrO/Sr(OH)₂ at the surface based on
11
12 88 different binding energies found for Sr 3d electrons using XPS. Nonetheless, by XPS
13
14 89 it is non-trivial to qualitatively (and almost impossible to quantitatively) deconvolute Sr
15
16 90 surface species from Sr in the LSC lattice. Accordingly, additional analytical methods
17
18 91 with complementary information content, e.g. not only on ionic binding situations but
19
20 92 also on phases, are therefore highly desirable.

21
22
23 93 Recently, Kubicek et al. ²¹ presented a novel tool for surface chemistry
24
25 94 analysis to overcome limitations of conventional depth profiling techniques. There,
26
27 95 the surface of LSC thin films was etched with dilute HCl, and the eluate containing
28
29 96 the dissolved cations was then analyzed on-line by ICP-OES. In contrast to classic
30
31 97 batch-wise extraction procedures, this approach provides time resolved information
32
33 98 on the availability and solubility of any dissolved species. Application of a slightly
34
35 99 modified etching procedure allowed the verification of a Sr enriched region at the
36
37
38 100 surface of porous LSC thin films ²⁴. However, limitations in sensitivity and
39
40 101 reproducibility of analysis prevented the determination of surface cation stoichiometry
41
42 102 as well as the measurement of dense LSC thin films. Thus, further methodological
43
44 103 development of the dynamic etching procedure is compulsory; in particular, to enable
45
46 104 the investigations required for a better understanding of Sr segregation and the
47
48 105 underlying physical and chemical phenomena.
49
50

51
52 106
53
54 107 In the present study we show how this approach with dynamic etching can be
55
56 108 continuously optimized. With the use of ICP-MS for element-selective on-line
57
58 109 detection significant improvements in sensitivity were achieved. Adaption of the flow-

1
2
3 110 injection system allowed consecutive etching of the sample with different solutions,
4
5 111 thereby enabling a differentiation between water soluble and acid soluble LSC
6
7 112 constituents. Moreover, improvements in accuracy and reproducibility of analysis
8
9 113 could be obtained by changing material, design and volume of the etching cartridge.
10
11 114 Achieved advancements allowed reliable measurement of the LSC thin film surface
12
13 115 and near-surface cation composition, providing quantitative information about
14
15 116 changes in the LSC stoichiometry. Applicability of the developed procedure for the
16
17 117 analysis of dense LSC thin films was demonstrated by excellent agreement of the
18
19 118 findings with results from low-energy ion scattering (LEIS) measurements.
20
21
22
23
24

25 120 **EXPERIMENTAL**

27 121 **Reagents and standard solutions**

28
29 122 High purity water was prepared using an Easypure water system (Thermo,
30
31 123 USA, resistivity 18 M Ω cm) and used throughout the entire study. Nitric acid (65 %)
32
33 124 and hydrochloric acid (37 %) was purchased from Merck (Darmstadt, Germany) with
34
35 125 p.a. grade. Certified stock solutions (1000 mg L⁻¹) of La, Sr and Co as well as Cu and
36
37 126 Mn were procured from Merck (Darmstadt, Germany) and used for the preparation of
38
39 127 calibration standards or as internal standards by dilution with 0.012 mol L⁻¹ HCl.
40
41
42
43
44

45 129 **Sample synthesis and preparation**

46
47 130 The LSC target for PLD was obtained from stoichiometric mixtures of La₂O₃,
48
49 131 SrCO₃, Co (99.995% Trace Select, Sigma Aldrich, Steinheim, Germany) powders
50
51 132 and prepared by Pechini synthesis²⁵ as described in Ref.²⁴. LSC thin films with a
52
53 133 thickness of 200 nm were deposited onto (100) oriented 9.5 mol% yttria stabilized
54
55 134 zirconia (YSZ) substrates (5x5x0.5 mm³) the deposition procedure and parameters
56
57 135 are given in Ref.²⁶.
58
59
60

136

137 **Instrumentation**

138 An iCAP 6500 series ICP-OES spectrometer (Thermo Scientific, USA) was
139 used for method development. Sample introduction was performed using an APEX E
140 high efficiency sample introduction system with a Meinhard concentric nebuliser and
141 a cyclonic spray chamber (ESI Elemental Scientific, USA). Instrumental parameters
142 used for ICP-OES measurement of thin surface layers are summarized in Table 1.
143 ICP-MS analysis was conducted using quadrupole instrumentation (Thermo iCAP
144 Qc, Thermo Scientific, Bremen, Germany). Sample introduction was accomplished
145 employing a Peltier-cooled spray chamber equipped with a concentric quartz glass
146 nebulizer. The instrumental parameters (Table 2) were optimized for maximum ^{115}In
147 signal and a $^{140}\text{Ce}^{16}\text{O}/^{140}\text{Ce}$ ratio below 1.9% on a daily basis using a standard tuning
148 solution. The amount of doubly charged ions was measured by the $^{137}\text{Ba}^{++}/^{137}\text{Ba}^{+}$
149 ratio which was below 3% for all experiments. To minimize the influence of potential
150 instrument induced artifacts, the sample signals were normalized using ^{55}Mn as
151 internal standard. Signal quantification was based on external calibration with
152 aqueous standard solutions. Standards and blanks were measured at the beginning,
153 during and at the end of an experimental session.

154 For analysis of time resolved etching profiles a flow-injection (FI) system
155 coupled to an ICP-OES or ICP-MS for element selective on-line detection was used.
156 The applied FI-system consisted of a six port injection valve (VICI, Cheminert C22,
157 USA) equipped with a sample cartridge for insertion of LSC samples. Arrangement of
158 the applied FI-manifold was similar to the one recently described by Limbeck et al.²⁷
159 for the dynamic extraction of water soluble trace metals in airborne particulate matter
160 (Fig. 1). In the first part of the work, commercially available Chromafix® SPE columns
161 (Macherey-Nagel, Germany, diameter 12 mm, length 14 mm) equipped with porous

1
2
3 162 quartz frits were employed as sample cartridges. In the final procedure, homemade
4
5 163 polytetrafluoroethylene (PTFE) micro-cartridges were used. In both cases the
6
7 164 cartridges were connected to the FI-system using conventional luer-fittings, which
8
9 165 allowed an easy and fast replacement of the etching compartment. The connections
10
11 166 between the individual parts of the FI-system were made with PTFE tubes having an
12
13 167 inner diameter of 0.7 mm.

14
15
16 168 LEIS analysis of the LSC thin films were performed using a Qtac100
17
18 169 spectrometer (ION-TOF GmbH, Germany) fitted with a high brightness ion source to
19
20 170 provide the primary beam (Hyperion, Oregon Physics, USA). Major advantage of
21
22 171 LEIS is that the analyzer beam only probes the first atomic layer. The elemental
23
24 172 composition of the surface was analyzed using a 6 keV Ne⁺ beam, which was
25
26 173 directed normal to the surface and the kinetic energy distribution of the backscattered
27
28 174 ions at 145° (collected over the entire azimuth) was analyzed to obtain the elemental
29
30 175 composition of the first monoatomic layer. For depth profiling, a 1 keV Ar⁺ sputtering
31
32 176 beam at a sputtering angle of 59 degrees was used. The sputtered area was 1.3 x
33
34 177 1.3 mm², with the central region of 1x1 mm² analyzed by the primary beam. The
35
36 178 sputter rate for the depth calibration of the profiles was estimated by measuring the
37
38 179 depth of a 300 x 300 μm² crater using laser interferometry (LEXT OLS4000,
39
40 180 Olympus, Japan), assuming that the rate was uniform for the LSC thin film. For the
41
42 181 quantification of the cation surface coverage, the plateau signals at the end of the
43
44 182 depth profiles were used as the reference value for the bulk stoichiometry, as
45
46 183 described in Ref. ²⁸.

47
48
49
50
51 184 To measure the impedance of LSC electrodes, a second LSC thin film (same
52
53 185 deposition conditions) was deposited on the back side of the YSZ substrate. The
54
55 186 impedance was then measured by a Novocontrol Alpha A High Performance
56
57
58
59
60

1
2
3 187 Frequency Analyzer with an alternating voltage of 10 mV (rms) in a frequency range
4
5 188 of 10^6 to 10^{-2} Hz. A detailed description of the setup can be found in Ref. ²⁶
6

7 189

8
9
10 **190 Dynamic etching procedure with on-line ICP-OES or ICP-MS detection**

11 The procedure starts with switching the valve in the load position, in this
12 alignment the etching solution (water or dilute HCl including 1.0 mg L^{-1} Cu used as
13
14 192 internal standard; flow rate 0.8 mL min^{-1}) is directed straight to the mixing device,
15
16 193 enabling the removal or insertion of a sample containing etching cartridge. Prior to
17
18 194 sample insertion the cartridge was carefully cleaned in an ultrasonic bath of 0.24 mol
19
20 195 L^{-1} HCl for 5 minutes to remove impurities remaining from the last measurement.
21
22 196 After integration of a sample containing cartridge, the valve is switched back into the
23
24 197 inject position and ICP-OES measurement is started. The etching solution introduced
25
26 198 into the etching compartment initiates the etching process of the LSC film. The
27
28 199 material dissolved by the etching agent is transported to the mixing device, where the
29
30 200 eluate is combined with a make-up solution (0.24 mol L^{-1} HCl containing 0.5 mg L^{-1}
31
32 201 Mn as additional internal standard; flow rate 0.6 mL min^{-1}) and mixed thoroughly. The
33
34 202 combined liquid flow is then directed into the sample introduction system of the ICP-
35
36 203 OES instrument, where the transient elution profiles are measured.
37
38 204

39
40
41
42
43 205 In case of more sensitive ICP-MS detection time resolved intensities for the
44
45 206 investigated isotopes were recorded with Qtegra software and exported as .csv files
46
47 207 for further data treatment, in particular internal standard correction to overcome
48
49 208 potential non-spectral interferences. For interpretation and further discussion the
50
51 209 intensity data derived from the etching experiments were converted into absolute
52
53 210 masses, which have been removed from the sample surface per time unit. For this
54
55 211 purpose calibration functions were determined by analyzing matrix adjusted standard
56
57 212 solutions with the same instrumental setup. Standards containing defined amounts of
58
59
60

1
2
3 213 the investigated elements (blank level up to contents of 1000 $\mu\text{g L}^{-1}$) and 10 $\mu\text{g L}^{-1}$
4
5 214 Cu (used as internal standard) were prepared just before use by appropriate dilution
6
7 215 of respective stock solutions with 0.012 mol L^{-1} HCl. For analysis, the etching solution
8
9 216 used as carrier was replaced with the standard solution to be investigated.
10
11 217 Measurement of those standard solutions was performed in the load position solely.
12
13 218 In analogy to the analysis of LSC samples, the liquid flow leaving the FI-manifold was
14
15 219 mixed with make-up solution; and the combined flow introduced into the detection
16
17 220 system. Prior to each ICP-MS analysis the system was purged with the examined
18
19 221 standard solution for approximately 30s, afterwards the signals of the selected
20
21 222 isotopes were monitored for 120s. The signal intensities (in counts per second)
22
23 223 obtained for the investigated analytes were normalized using Mn as internal standard
24
25 224 and correlated with the injected analyte masses, showing for all elements a linear
26
27 225 behavior throughout the investigated mass range.
28
29
30
31
32

226

227 **RESULTS**

228 **Method development**

229 Limitations in reproducibility and accuracy of analysis are considered the main
30
31 230 drawbacks of the procedure reported in Ref. ²¹. Typical sources for these problems
32
33 231 are analyte losses and/or memory effects, changes in the carrier flow rate and/or
34
35 232 composition, alterations in the nebulizer efficiency as well as variations in the plasma
36
37 233 load, causing undesirable fluctuations in the measured signal intensities. Since the
38
39 234 investigated elements provide an enhanced solubility at lower sample pH, adsorption
40
41 235 losses and/or memory effects are only of concern when pure water is applied as
42
43 236 etching agent. In the latter case, material dissolved from the LSC surface could be
44
45
46
47
48
49
50
51
52 237 lost during transport from the sample cartridge into the plasma due to adsorption of
53
54
55
56
57
58 238 dissolved material on different parts of the analytical system (tubings, nebulizer,
59
60

1
2
3 239 spray chamber, torch), impeding an accurate measurement of the eluate
4
5 240 composition. To minimize the risk of analyte losses and/or memory effects, the
6
7 241 sample flow coming from the etching cartridge is mixed on-line with 0.24 mol L⁻¹ HCl
8
9 242 as a make-up solution. The combined liquid flow is then introduced into the nebulizer
10
11 243 unit of the detecting ICP-OES, where the transient etching profiles are measured.

12
13
14 244 To overcome the difficulties related with the mentioned non-spectral
15
16 245 interferences, internal standards were applied. Whereas errors related to the sample
17
18 246 introduction system could be compensated with any internal standard, the accurate
19
20 247 correction of plasma related effects (e.g. energy transfer) requires the use of
21
22 248 elements with excitation and ionization energies comparable to that of the target
23
24 249 analytes. Thus, the elements Cu and Mn were selected as internal standards, having
25
26 250 emission wavelengths close to that of the investigated LSC constituents. With the
27
28 251 use of Mn (constituent of the make-up solution) changes in the sample introduction
29
30 252 efficiency as well as plasma load could be monitored and corrected if necessary. Cu
31
32 253 as constituent of the etching solution is used to control the liquid flow directed
33
34 254 through the FI-manifold including the etching compartment. Moreover, the
35
36 255 homogeneity of the solution leaving the mixing device could be controlled, a
37
38 256 prerequisite for the accurate and reproducible measurement of etching profiles.

39
40
41
42
43 257 Beside improvement of the measurement step, a continuous optimization of
44
45 258 the LSC thin film etching process is also required for reliable determination of
46
47 259 distribution profiles. For this purpose an etching compartment is mandatory which
48
49 260 delivers the eluent to the whole thin film surface uniformly, enabling homogenous
50
51 261 sample dissolution by the eluent. Moreover, the etching compartment should provide
52
53 262 fast wash out times to avoid mixing of sample eluates from successive sample
54
55 263 depths, and the absence of any memory effects due to adsorption or release of
56
57 264 analytes. The last issue is of special importance since the acidic make-up solution

1
2
3 265 introduced to overcome the problem of analyte losses (see previous section) protects
4
5 266 only the sample introduction system located behind the mixing device. Thus in the
6
7 267 etching cartridge adsorption losses are still possible, since this part is positioned
8
9 268 before the mixing device and therefore operated with etching solution only.

10
11 269 In the very first part of this work, where LSC thin films were simply sandwiched
12
13 270 between two porous quartz frits and inserted into a SPE cartridge as reported by
14
15 271 Kubicek et al. ²¹, differentiation between water soluble and acid soluble contents of
16
17 272 LSC thin films was hampered. Memory-effects caused by the pH dependent
18
19 273 adsorption/desorption of dissolved LSC constituents on the porous frits were found to
20
21 274 be the main reason. To overcome the problems associated with the use of
22
23 275 commercial SPE cartridges and porous frits as sample holders, a new etching
24
25 276 compartment was manufactured, which allows fixation of the LSC sample without the
26
27 277 use of any additional substrate. The material chosen for this application was PTFE,
28
29 278 giving the advantage of being resistant to strong acids and acetone, which also
30
31 279 enables an effective cleaning of the cartridge prior to next use. Particular emphasis
32
33 280 was laid on the geometry of the etching compartment (for details see Fig. 2), which
34
35 281 should prevent movement of the sample during the etching process. The square
36
37 282 sample (5x5 mm²) is placed in the funnel shaped etching compartment (corners in
38
39 283 contact with the wall) and the liquid can pass the sample along the edges. Moreover,
40
41 284 the volume of the compartment was minimized from 984 μ L to 289 μ L to decrease
42
43 285 wash out time, hence lowering peak broadening. With this set-up reproducibility of
44
45 286 analysis was improved significantly, since memory effects as well as unexpected
46
47 287 fluctuations in the liquid flow could be completely avoided, enabling a reproducible
48
49 288 determination of water and acid soluble LSC constituents.
50
51
52
53
54
55
56
57
58
59
60

290 **Element selective detection using ICP-MS**

291 As demonstrated in Ref. ²¹ the detection power of the ICP-OES employed as
292 detection system is sufficient for the analysis of porous LSC films, but in case of
293 dense LSC films with lower surface area limitations in sensitivity are expected.
294 Compared to porous LSC films, the decreased surface area of dense LSC films
295 results in a reduction of the etching rate, thus the amount of analyte introduced into
296 the ICP per time unit is lower, impeding accurate analysis of the derived eluate.
297 Insufficient detection power hampers also an appropriate characterization of the
298 water soluble LSC phase, thus the stoichiometry determined for the water soluble
299 phase could be erroneous. To overcome the problems related with ICP-OES
300 detection, in all further experiments solely ICP-MS was used for element selective
301 analysis. However, compared to ICP-OES the operating conditions of ICP-MS are
302 different, thus, adaption of the dynamic etching procedure was necessary. In a first
303 step the flow rates of etching and make-up solution were optimized, main purpose of
304 this optimization step was to improve sample introduction efficiency without any
305 deterioration of the etching profiles. Best results were achieved with a combined
306 liquid flow of 1.0 mL min⁻¹. For lower flow rates, a further increase in the sensitivity of
307 ICP-MS analysis was observed, but the wash-out behavior of the etching
308 compartment decreased distinctly. The internal standards selected for ICP-OES
309 measurements were also applicable for detection with ICP-MS, since the ionization
310 potentials of the target analytes are comparable (Co) or even lower (La, Sr) to that of
311 the internal standard elements (Cu, Mn). Furthermore, ICP-MS analysis of etching
312 and make-up solution delivered basically no signals on the m/z values used for
313 detection of target analytes, indicating the absence of notable contaminations as well
314 as spectral interferences. Concentrations of the applied internal standards were
315 reduced to 10 µg L⁻¹ (Cu) and 5 µg L⁻¹ (Mn) only.

1
2
3 316 With the optimized flow rate and the instrumental parameters described in
4
5 317 Table 2 a significant increase in sensitivity could be achieved. For signal
6
7 318 quantification matrix adjusted standard solutions and integration intervals of 1 s were
8
9 319 applied, a more detailed description is presented in the experimental section.
10
11 320 Compared to ICP-OES, the detection limits ranging from 7 (La at 379.478 nm) to 35
12
13 321 (Co at 228.696 nm) $\mu\text{g L}^{-1}$ could be reduced by 2 magnitudes of order using the ICP-
14
15 322 MS ($0.03 \mu\text{g L}^{-1}$ for ^{139}La , $0.04 \mu\text{g L}^{-1}$ for ^{59}Co and $0.15 \mu\text{g L}^{-1}$ for ^{86}Sr). With
16
17 323 quadrupole ICP-MS instrumentation lower detection limits are usually possible,
18
19 324 however, the operating conditions required in this special application (sample uptake
20
21 325 rate of 1.0 mL min^{-1} , and the measurement of transient signals with integration
22
23 326 intervals of 1 s only) resulted in decreased sensitivity. The quality of the applied
24
25 327 chemicals could also contribute to the achieved detection limits, since prevailing
26
27 328 impurities might increase the background signals for the target analytes. Thus, with
28
29 329 the use of ultrapure grade chemicals further improvements in sensitivity are
30
31 330 expected. Nevertheless, the detection limits were low enough to quantify the
32
33 331 transient data obtained during each step of the etching process. Fig. 3 shows
34
35 332 element intensity/time profiles of an LSC thin film first etched with water and then
36
37 333 with 0.012 mol L^{-1} HCl measured by ICP-MS. The ^{86}Sr baseline signals were found
38
39 334 to be in the order of 200 cps only, whereas the signal intensity increases to 200.000
40
41 335 cps during water etching before it slowly diminishes to around 2.000 cps and rises
42
43 336 again to around 150.000 cps after switching the eluent to diluted HCl. Using the
44
45 337 determined calibration functions derived ICP-MS signals were converted into
46
47 338 concentrations, which were found to range between some $\mu\text{g l}^{-1}$ and several hundred
48
49 339 $\mu\text{g L}^{-1}$.
50
51
52
53
54
55
56
57
58
59
60

1
2
3 341 **Analytical performance**
4

5 342 As already mentioned in the introduction, changes of the surface cation
6
7 343 stoichiometry are considered the main reason for degradation of the electrochemical
8
9 344 performance of LSC. Thus, special emphasis was dedicated to the reliable analysis
10
11 345 of surface and near-surface regions of LSC thin films. For this purpose, a set of LSC
12
13 346 thin films was produced using identical PLD conditions. Analysis of water soluble
14
15 347 parts of the films was performed with the use of water as etching solution; samples
16
17 348 were subsequently treated with 0.012 mol L⁻¹ HCl to continuously dissolve the
18
19 349 remaining acid soluble LSC constituents. Progress of the etching process was
20
21 350 monitored by ICP-MS measurement of the derived sample eluates. Obtained etching
22
23 351 profiles do not reveal any obvious differences, indicating that the measurement of
24
25 352 LSC thin films is highly reproducible. This is also confirmed by the small variations in
26
27 353 the peak areas obtained for the water soluble LSC parts, showing relative standard
28
29 354 deviations (n=3) of 1.0% for Sr, 1.6% for La and 3.0% for Co. Similar findings can be
30
31 355 found in literature for other FI-ICP-MS procedures reported for a variety of
32
33 356 applications including on-line sample extraction ²⁹, analyte enrichment ³⁰ and matrix
34
35 357 or analyte separation ³¹.
36
37
38
39

40 358 Due to the higher sensitivity of the ICP-MS employed as detection system,
41
42 359 experiments become feasible which were not possible with the setup described in
43
44 360 Ref. ²¹. One scientific task which could thus be addressed is the analysis of dense
45
46 361 LSC thin films using water as etching solvent. This results in very low etching rates
47
48 362 and thus sample eluates with concentrations not measurable with ICP-OES. To this
49
50 363 end, a set of identical dense LSC thin film samples was investigated by means of
51
52 364 both detection techniques and treated first with water and subsequently with etching
53
54 365 solutions of increased acidity. For further discussion, the intensity/time data received
55
56 366 by the detector was converted into molar ratios versus time profiles using the
57
58
59
60

1
2
3 367 procedure developed for signal quantification. As expected, the ICP-OES signals
4
5 368 were close to the respective detection limits, and do not allow a reliable differentiation
6
7 369 between parts of LSC with different solubility. Detection by ICP-MS, on the other
8
9 370 hand, leads to very precise and reliable profiles for all elements (Fig. 4a). From the
10
11 371 ICP-MS results, it is evident that significant quantities of Sr but also Co and La were
12
13 372 dissolved by the treatment with water. Moreover, the amount of water soluble species
14
15 373 at the thin film surface decreased significantly with ongoing reaction time, see also
16
17 374 Fig. 3. Changing the eluent to 0.012 mol L⁻¹ HCl resulted in substantially increased
18
19 375 signals for Sr, Co and La, until a horizontal plateau of signals (Fig. 3) as well as
20
21 376 molar ratios (Fig. 4a) is observed, indicating a constant etching rate for all thin film
22
23 377 constituents.

24
25
26
27 378 From the findings presented in Fig. 4a, it can be concluded that the near
28
29 379 surface region of the LSC thin film contains mainly Sr, while Co and La were only
30
31 380 detected in minor amounts. While with ongoing etching time and thus sample depth
32
33 381 the absolute ICP-MS signals decreased drastically, the relative contribution of Co
34
35 382 and La increased continuously, leading to a rather constant composition of the water
36
37 383 soluble part of the LSC sample after approximately 200 s. Compared to the known
38
39 384 LSC thin film stoichiometry (dotted line in Fig. 4a) this water soluble fraction
40
41 385 (between 200 s - 400 s) still exhibits significant differences – in particular a depletion
42
43 386 of La and an enhanced contribution of Sr. However, only a very small amount of
44
45 387 cations (< 0.3 nmol) is dissolved during this time interval, which is also reflected by
46
47 388 the tailing of the water-soluble peak in Fig. 3. With the use of 0.012 mol L⁻¹ HCl as
48
49 389 etching solution the detected molar ratio changed again, revealing practically the
50
51 390 known composition of the LSC thin films.

52
53
54
55
56 391 Further information becomes available when relating the molar ratios to the
57
58 392 total amount of eluted cations instead of time. It can be clearly deduced from the ICP-

1
2
3 393 MS results (Fig. 4b), that the water soluble fraction represents only a minor part of
4
5 394 the dissolved LSC thin film sample and is largely Sr enriched. Assuming that the LSC
6
7 395 sample is dissolved homogeneously (layer by layer) the obtained concentration
8
9 396 versus time plots could even be converted into depth profiles with knowledge of the
10
11 397 respective etching rates. Application of this methodology would result in depth
12
13 398 resolutions reaching the sub-nm range (see top abscissa in Fig. 4b) and thus be very
14
15 399 competitive to traditional approaches such as GDMS ³², SIMS ³³ or LA-ICP-MS
16
17 400 analysis ³⁴. However, since preferential dissolution of the LSC thin film material on
18
19 401 grain boundaries or defect rich regions will most probably occur, the depth scale
20
21 402 should only be considered as a rough estimation.
22
23
24

25 403 For demonstration of accuracy and reproducibility four PLD deposition batches
26
27 404 of LSC thin films, consisting of four individual samples each (i.e. 16 samples), were
28
29 405 either analyzed using the procedure developed or in a conventional batch wise
30
31 406 approach by dissolving the entire film. For both procedures, 0.012 mol·l⁻¹ HCl was
32
33 407 chosen as etching solution. The analysis time for the dynamic measurements was
34
35 408 extended accordingly to allow monitoring of the whole dissolution process, signal
36
37 409 quantification was performed as mentioned before. For batch wise experiments the
38
39 410 samples were treated with the etching solution in closed reaction tubes. After
40
41 411 complete dissolution of the LSC thin films, the substrates were removed from the
42
43 412 tubes and sample acidity of the derived solutions has been adjusted to 0.12 mol·l⁻¹
44
45 413 HCl prior to ICP-MS analysis. The results derived for the total cation amounts of the
46
47 414 LSC samples were in excellent agreement, revealing only negligible differences
48
49 415 between batch experiments and dynamic ICP-MS measurements. Furthermore, for
50
51 416 quality assurance the samples derived from batch experiments were also measured
52
53 417 using ICP-OES, delivering results practically identical to the ICP-MS findings. Thus,
54
55 418 the applicability of the proposed dynamic etching procedure as well as the accuracy
56
57
58
59
60

1
2
3 419 of the applied quantification approach is confirmed, in particular when considering
4
5 420 that the production of LSC thin films can also generate minor variations in the
6
7 421 composition of the investigated sample sets.
8

9 422

10
11 423 **Analysis of the near surface region of different LSC thin films and comparison**
12
13 424 **with LEIS measurements**

14
15
16 425 The developed procedure was applied to compare the surface composition of
17
18 426 different dense LSC thin films. In order to understand which parts of the films are
19
20 427 water soluble and to compare these results to LEIS measurements, the following
21
22 428 experiment was performed: Three of six as-deposited LSC thin films were stirred ex-
23
24 429 situ for 10 minutes in ultrapure H₂O and blown dry with high purity N₂. All six thin
25
26 430 films were then analyzed by the dynamic ICP-MS etching procedure. Representative
27
28 431 time-resolved concentration profiles for all elements are shown in Fig. 5a and 5b. The
29
30 432 only significant difference between the as-deposited and H₂O pretreated thin films is
31
32 433 seen in the part of the profile resulting from H₂O etching.
33
34

35
36 434 The exact amount of cations etched by water were determined by integration
37
38 435 (Fig. 5 beginning of the measurement up to the dashed line). The amount of water
39
40 436 soluble Sr is decreased by 0.39 ± 0.02 nmol after the H₂O pretreatment, while only
41
42 437 minor changes are observed in the La and Co concentration. From the lattice
43
44 438 parameter of SrO, it can be calculated that 0.33 nmol Sr would be needed to form
45
46 439 one atomic layer of highly water-soluble SrO (100 direction) covering the entire 5x5
47
48 440 mm² surface of the thin film. Accordingly, the additional 0.39 nmol Sr removed from
49
50 441 LSC layers without H₂O pretreatment corresponds to approximately 1.2 atomic layers
51
52 442 of SrO. The remaining cations dissolved with as well as without H₂O pretreatment
53
54 443 would then sum up to about one to two slightly Sr enriched elementary cells of LSC,
55
56 444 though inhomogeneous etching might play a role here. This result strongly suggests
57
58
59
60

1
2
3 445 that the main difference between the surface composition of an as-deposited and a
4
5 446 H₂O treated layer is the absence of a strongly Sr-rich layer in the latter case. The fact
6
7 447 that also after H₂O pretreatment, in the beginning of the measurement, an increased
8
9 448 amount of the LSC lattice is dissolved in water may be explained with the influence of
10
11 449 trace gases, e.g. CO₂, SO₂ adsorbed at the sample surface or PTFE compartment.
12
13

14 450 To confirm the findings from ICP-MS measurements, further LSC thin films
15
16 451 were prepared and analyzed by LEIS. Depth profiles over the first 5 nm of the thin
17
18 452 films for the Sr/(Sr+La) and Co/(Sr+La) ratio are shown in Fig. 6a and 6b,
19
20 453 respectively. The very first measurement points of the LEIS profiles represent the
21
22 454 cation composition of the surface layer. For the as-deposited thin film it can be seen
23
24 455 that most of the cation sites in the surface layer are occupied by Sr (81%), Co and La
25
26 456 are thus strongly depleted. An enrichment in Sr and depletion of La is also
27
28 457 determined for the first 2 – 3 nm of the LSC thin film, even though the sub-surface
29
30 458 shows a Co / (Sr + La) ratio that is already very close to the bulk stoichiometry. After
31
32 459 the ex-situ H₂O treatment, the surface layer shows a decreased Sr / (Sr + La) ratio
33
34 460 compared to the as-deposited sample, although Co is still depleted. A slight Sr
35
36 461 enrichment is again observed beneath the surface.
37
38
39

40 462 First, a very good qualitative agreement is thus found between the LEIS
41
42 463 results at the surface and the water-soluble amount of cations determined by ICP-
43
44 464 MS. Both methods suggest that the LSC lattice has a very Sr rich termination layer. A
45
46 465 Sr enriched near-surface region (1-3 nm information depth) was also confirmed by
47
48 466 Cai et al.²³ from XPS measurements on similar LSC thin films. In their work, they
49
50 467 also proposed that the LSC lattice is SrO / Sr(OH)₂ terminated, since evidence of
51
52 468 SrCO₃ species was not obtained. Also the La enriched and Co depleted surface
53
54 469 composition measured by our LEIS study after the ex-situ H₂O treatment finds its
55
56 470 counter-part in the ICP-MS experiment: A sharp peak of La together with a depletion
57
58
59
60

1
2
3 471 of Co is observed after switching from H₂O to diluted hydrochloric acid (Fig. 5b and
4
5 472 5d).

6
7 473 Quantitatively, LEIS results indicate a Sr coverage of 81% of the surface. ICP-
8
9 474 MS, on the other hand, revealed 1.2 atomic layers of SrO. This difference may arise
10
11 475 since LEIS probes a 2D projection of the surface and ICP-MS the true surface area
12
13 476 (total solid-gas phase boundary) of the sample. The latter is larger due to cracks in
14
15 477 the films. In a previous work we were able to show on microporous LSC thin films
16
17 478 that the enhanced surface area from open porosity can be even quantified from the
18
19 479 water-soluble amount of Sr²⁵.

20
21
22
23 480 Finally, EIS measurements were conducted on as-deposited and H₂O
24
25 481 pretreated samples at 400°C in 1 mbar pO₂ in order to compare the electrochemical
26
27 482 properties (O₂ exchange kinetics); representative spectra are shown in Fig. 7. A
28
29 483 detailed analysis of such impedance data is given in Ref. ³⁵ and showed that the low
30
31 484 frequency arc can be correlated to the oxygen exchange reaction at the LSC surface.
32
33 485 It can be seen that the surface treatment does not affect the electrolyte resistance
34
35 486 but lowers the electrode resistance by about 50%. This confirms the detrimental
36
37 487 effect of the water-soluble SrO top layer on the oxygen exchange activity.
38
39
40
41 488

42 43 489 **CONCLUSIONS**

44
45 490 The analytical procedure presented in this work allows the chemical
46
47 491 composition of surface and near surface regions of complex metal oxide thin films to
48
49 492 be determined. Differentiation between water and acid soluble sample constituents
50
51 493 was accomplished by preliminary treatment of the sample surface with water,
52
53 494 followed by etching with diluted HCl, and element specific on-line analysis of the
54
55 495 derived solutions. The required sensitivity was achieved with the use of ICP-MS as
56
57 496 detection technique; non-spectral interferences during on-line ICP-MS measurement
58
59
60

1
2
3 497 were corrected by means of internal standards. Stepwise optimization of the etching
4
5 498 cartridge resulted in an improved washout behavior and the complete elimination of
6
7 499 memory effects. Compared to conventional approaches used for surface analysis of
8
9 500 solids such as XRF, SIMS, GDOES or GDMS, laser ablation combined with ICP-OES
10
11 501 or ICP-MS, the necessity of appropriate matrix matched standards could be
12
13 502 circumvented, since simple aqueous standards could be used for signal
14
15 503 quantification. A further benefit of the proposed procedure is the ability to distinguish
16
17 504 phases with different solubility, whereas common techniques allow only the
18
19 505 measurement of total element contents.
20
21

22
23 506 The developed procedure was applied for the analysis of LSC thin films. LEIS
24
25 507 and on-line ICP-MS measurements revealed a water-soluble Sr-rich termination layer
26
27 508 on freshly deposited dense LSC thin films. Qualitatively and quantitatively, a very
28
29 509 good agreement between the results obtained by these two techniques was found.
30
31 510 The oxygen exchange rates were measured by impedance spectroscopy and an
32
33 511 improvement was determined after removing the water-soluble Sr-rich phase from
34
35 512 the surface, suggesting that the LSC surface is blocked or inactivated by the
36
37 513 formation of this water soluble Sr-rich phase.
38
39

40
41 514

42 43 515 **ACKNOWLEDGEMENTS**

44
45 516 The authors gratefully acknowledge funding by Austrian Science Fund (FWF)
46
47 517 projects P21960-N17 and W1243. JAK, TI, HT and JD also acknowledge support
48
49 518 from the International Institute for Carbon Neutral Energy Research (wpi-I2CNER),
50
51 519 funded by the World Premier Research Center Initiative of the Ministry of Education,
52
53 520 Culture, Sports, Science and Technology. HT thanks the financial support from the
54
55 521 Japanese Society for Promotion of Science (JSPS postdoctoral fellowship and
56
57 522 Kakenhi Grant-in-Aid P13770).
58
59
60

523 REFERENCES

- 524 1. A. S. Bhalla, R. Guo and R. Roy, *Mat Res Innovat*, 2000, **4**, 3-26.
- 525 2. M. B. Gawande, R. K. Pandey and R. V. Jayaram, *Catalysis Science &*
526 *Technology*, 2012, **2**, 1113-1125.
- 527 3. I. E. Wachs, *Catalysis Today*, 2005, **100**, 79-94.
- 528 4. S. Royer, D. Duprez, F. Can, X. Courtois, C. Batiot-Dupeyrat, S. Laassiri and
529 H. Alamdari, *Chemical Reviews*, 2014, **114**, 10292-10368.
- 530 5. G. Friedbacher and H. Bubern, *Surface and Thin Film Analysis: A*
531 *Compendium of Principles, Instrumentation, and Applications, Second Edition*,
532 2011.
- 533 6. T. Nelis and J. Pallosi, *Applied Spectroscopy Reviews*, 2006, **41**, 227-258.
- 534 7. B. Fernández, R. Pereiro and A. Sanz-Medel, *Analytica Chimica Acta*, 2010,
535 **679**, 7-16.
- 536 8. J. Pisonero, J. Koch, M. Wälle, W. Hartung, N. D. Spencer and D. Günther,
537 *Analytical Chemistry*, 2007, **79**, 2325-2333.
- 538 9. B. Hattendorf, J. Pisonero, D. Günther and N. Bordel, *Analytical Chemistry*,
539 2012, **84**, 8771-8776.
- 540 10. W. Lee, J. W. Han, Y. Chen, Z. Cai and B. Yildiz, *Journal of the American*
541 *Chemical Society*, 2013, **135**, 7909-7925.
- 542 11. S. B. Desu and D. A. Payne, *Journal of the American Ceramic Society*, 1990,
543 **73**, 3391-3397.
- 544 12. H. Wang, Y. Zhu, R. Tan and W. Yao, *Catalysis Letters*, 2002, **82**, 199-204.
- 545 13. A. Yan, V. Maragou, A. Arico, M. Cheng and P. Tsiakaras, *Applied Catalysis*
546 *B: Environmental*, 2007, **76**, 320-327.
- 547 14. Y. Nishihata, J. Mizuki, T. Akao, H. Tanaka, M. Uenishi, M. Kimura, T.
548 Okamoto and N. Hamada, *Nature*, 2002, **418**, 164-167.
- 549 15. W. Kobsiriphat, B. D. Madsen, Y. Wang, M. Shah, L. D. Marks and S. A.
550 Barnett, *Journal of The Electrochemical Society*, 2010, **157**, B279-B284.
- 551 16. S. B. Adler, *Chemical reviews*, 2004, **104**, 4791-4844.
- 552 17. R. M. Ormerod, *Chemical Society Reviews*, 2003, **32**, 17-28.
- 553 18. F. Zhao, R. Peng and C. Xia, *Fuel Cells Bulletin*, 2008, **2008**, 12-16.
- 554 19. H. Yokokawa, H. Tu, B. Iwanschitz and A. Mai, *Journal of Power Sources*,
555 2008, **182**, 400-412.
- 556 20. V. I. Sharma and B. Yildiz, *Journal of The Electrochemical Society*, 2010, **157**,
557 B441-B448.
- 558 21. M. Kubicek, A. Limbeck, T. Fromling, H. Hutter and J. Fleig, *Journal of The*
559 *Electrochemical Society*, 2011, **158**, B727-B734.
- 560 22. S. P. Simner, M. D. Anderson, M. H. Engelhard and J. W. Stevenson,
561 *Electrochemical and Solid-State Letters*, 2006, **9**, A478-A481.
- 562 23. Z. Cai, M. Kubicek, J. Fleig and B. Yildiz, *Chemistry of Materials*, 2012, **24**,
563 1116-1127.
- 564 24. G. M. Rupp, A. Limbeck, M. Kubicek, A. Penn, M. Stoger-Pollach, G.
565 Friedbacher and J. Fleig, *Journal of Materials Chemistry A*, 2014, **2**, 7099-
566 7108.
- 567 25. M. P. Pechini, 1967, **US3330697 A**.
- 568 26. G. M. Rupp, A. Schmid, A. Nennung and J. Fleig, *Journal of The*
569 *Electrochemical Society*, 2016, **163**, F564-F573.
- 570 27. A. Limbeck, C. Wagner, B. Lendl and A. Mukhtar, *Analytica Chimica Acta*,
571 2012, **750**, 111-119.

- 1
2
3 572 28. J. Druce, H. Tellez, M. Burriel, M. D. Sharp, L. J. Fawcett, S. N. Cook, D. S.
4 573 McPhail, T. Ishihara, H. H. Brongersma and J. A. Kilner, *Energy &*
5 574 *Environmental Science*, 2014, **7**, 3593-3599.
6 575 29. J. Buanuam, K. Tiptanasup, J. Shiowatana, M. Miro and E. Harald Hansen,
7 576 *Journal of Environmental Monitoring*, 2006, **8**, 1248-1254.
8 577 30. D. Das, M. Dutta, M. L. Cervera and M. de la Guardia, *TrAC Trends in*
9 578 *Analytical Chemistry*, 2012, **33**, 35-45.
10 579 31. P. Galler, A. Limbeck, S. F. Boulyga, G. Stingeder, T. Hirata and T. Prohaska,
11 580 *Analytical Chemistry*, 2007, **79**, 5023-5029.
12 581 32. J. Pisonero, N. Bordel, C. Gonzalez de Vega, B. Fernández, R. Pereiro and A.
13 582 Sanz-Medel, *Anal Bioanal Chem*, 2013, **405**, 5655-5662.
14 583 33. J. S. Fletcher and J. C. Vickerman, *Analytical Chemistry*, 2013, **85**, 610-639.
15 584 34. A. Gutierrez-Gonzalez, C. Gonzalez-Gago, J. Pisonero, N. Tibbetts, A.
16 585 Menendez, M. Velez and N. Bordel, *Journal of Analytical Atomic*
17 586 *Spectrometry*, 2015, **30**, 191-197.
18 587 35. G. M. Rupp, H. Tellez, J. Druce, A. Limbeck, T. Ishihara, J. Kilner and J. Fleig,
19 588 *Journal of Materials Chemistry A*, 2015, **3**, 22759-22769.
20
21
22
23
24
25
26
27
28
29
30
31
32
33
34
35
36
37
38
39
40
41
42
43
44
45
46
47
48
49
50
51
52
53
54
55
56
57
58
59
60

1
2
3 589 **Captions of Tables and Figures**

4
5 590 **Table 1** Instrumental parameters used for ICP-MS analysis

6
7 591 **Table 2** Instrumental parameters used for ICP-OES analysis

8
9 592

10
11 593 **Fig. 1** FI Manifold for dynamic etching of LSC thin film samples: P peristaltic pump, V
12 6-port valve.

13
14 594
15 595 **Fig. 2** PTFE etching compartment.

16
17 596 **Fig. 3** Time resolved ^{59}Co , ^{86}Sr , ^{139}La intensities of LSC thin films analyzed using
18 597 PTFE compartment and ICP-MS. The eluent was switched from ultrapure H_2O to
19 598 $0.012 \text{ mol}\cdot\text{l}^{-1}$ after $\sim 390 \text{ s}$.

20
21 599 **Fig. 4** (a) shows the molar ratio of dense LSC thin films vs. measurement time during
22 600 the dynamical etching procedure and analysis by ICP-MS, including description of
23 601 applied eluent sequence below the profiles. In (b) the molar ratio is plotted vs. the
24 602 total cation amount (similar to depth profiles).

25
26 603 **Fig. 5** Representative time-resolved ICP-MS concentration profiles for (a) as-
27 604 deposited LSC thin films and (b) after ex-situ H_2O treatment. Inset in (b) directly
28 605 compares the Sr concentration in the water-soluble part.

29
30 606 **Fig. 6** (a) Sr / (Sr + La) and (b) Co / (Sr + La) depth profiles measured by LEIS for
31 607 as-deposited and ex-situ H_2O treated LSC thin films.

32
33 608 **Fig. 7** Nyquist plots of the impedance measurements performed at 400°C in 1 mbar
34 609 pO_2 for as-deposited and H_2O treated LSC.

610 **Table 1** Instrumental parameters used for ICP-MS analysis

<i>ICP-MS instrumentation</i>	<i>Thermo iCAP Q</i>
total sample flow rate	0.8 mL min ⁻¹
nebulizer gas flow	0.8 L min ⁻¹
aux. gas flow	0.8 L min ⁻¹
cool gas flow	14 L min ⁻¹
RF power	1550 W
Cones	Ni
measured isotopes	⁵⁵ Mn, ⁵⁹ Co, ⁶³ Cu, ⁶⁵ Cu, ⁸⁶ Sr,
dwel time per isotope	0.010 s
mass resolution	m/Δm = 300

611

612

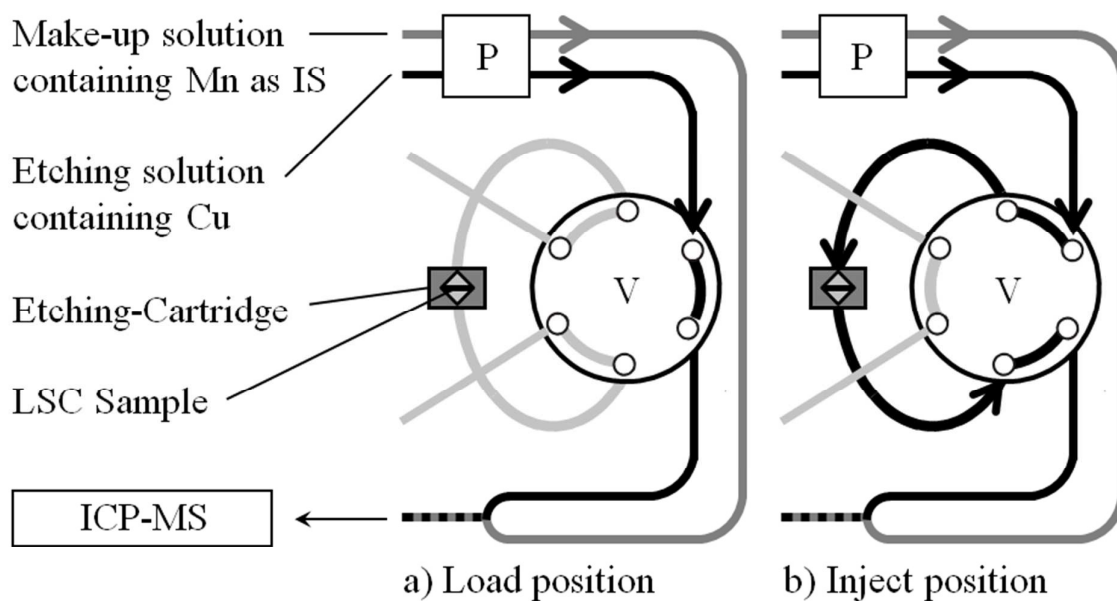
613 **Table 2** Instrumental parameters used for ICP-OES analysis

Parameter	Value	Parameter	Value
Rf power	1250 W	Nebulizer flow	0.70 l min ⁻¹
total sample flow rate	1.4 ml min ⁻¹	Auxiliary flow	0.8 l min ⁻¹
viewing height	12 mm	Coolant flow	12 l min ⁻¹
measurement mode:	transient signals with 1 s observation time per data point		
background correction:	constant shift from analytical line		
signal processing:	Thermo ITEVA software		
Element	λ ₁ [nm]	λ ₂ [nm]	λ ₃ [nm]
La	333.749	379.478	419.655
Sr	216.596	346.446	421.552
Co	228.696	238.892	
Cu	224.700	324.754	
Mn	257.610		

614

615

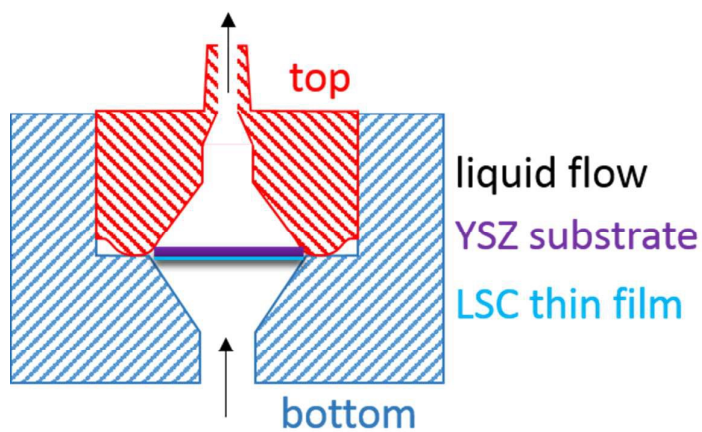
616



617

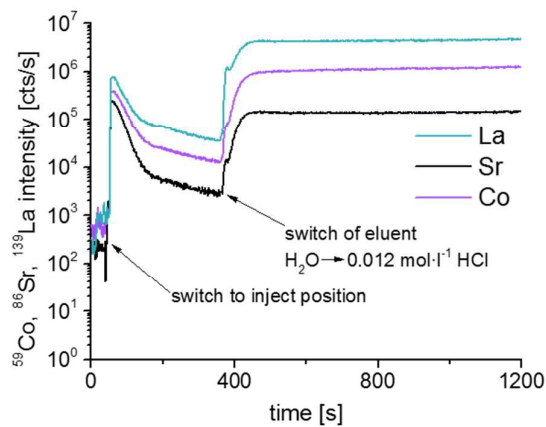
618 **Fig. 1** FI Manifold for dynamic etching of LSC thin film samples: P peristaltic pump, V

619 6-port valve.



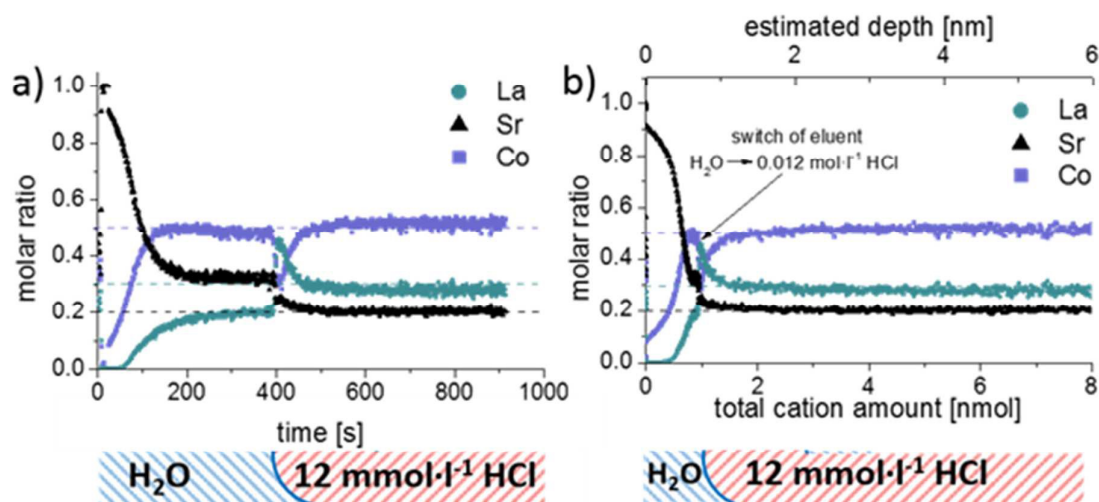
620

621 **Fig. 2** PTFE etching compartment.



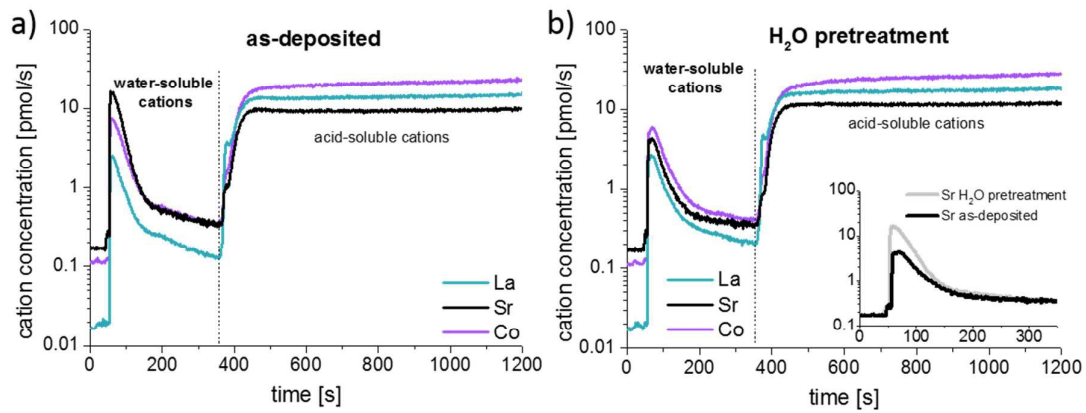
623 **Fig. 3** Time resolved ^{59}Co , ^{86}Sr , ^{139}La intensities of LSC thin films analyzed using
624 PTFE compartment and ICP-MS. The eluent was switched from ultrapure H_2O to
625 $0.012 \text{ mol}\cdot\text{l}^{-1}$ after $\sim 390 \text{ s}$.

626



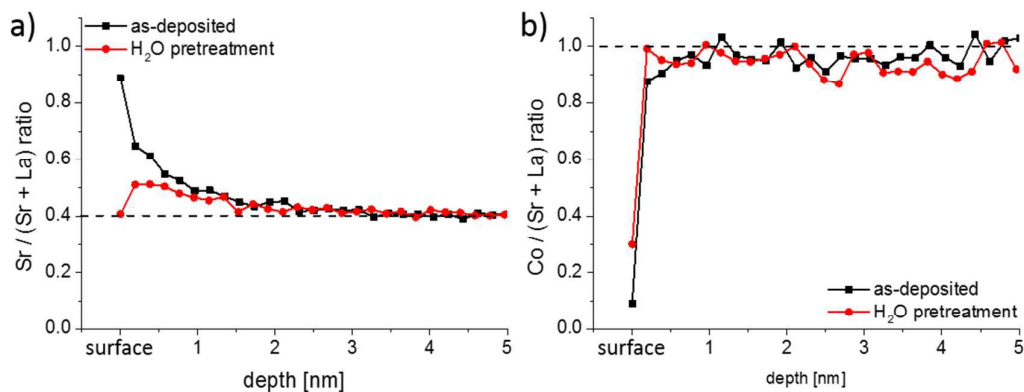
627

628 **Fig. 4** (a) shows the molar ratio of dense LSC thin films vs. measurement time during
 629 the dynamical etching procedure and analysis by ICP-MS, including description of
 630 applied eluent sequence below the profiles. In (b) the molar ratio is plotted vs. the
 631 total cation amount (similar to depth profiles).



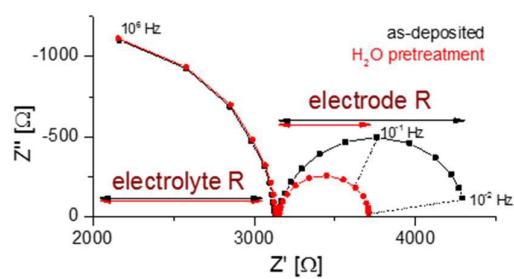
632

633 **Fig. 5** Representative time-resolved ICP-MS concentration profiles for (a) as-
634 deposited LSC thin films and (b) after ex-situ H₂O treatment. Inset in (b) directly
635 compares the Sr concentration in the water-soluble part.



636

637 **Fig. 6** (a) Sr / (Sr + La) and (b) Co / (Sr + La) depth profiles measured by LEIS for638 as-deposited and ex-situ H₂O treated LSC thin films.



639

640 **Fig. 7** Nyquist plots of the impedance measurements performed at 400°C in 1 mbar641 pO₂ for as-deposited and H₂O treated LSC.